

REFERENCES

1. G.T. Van de Roer, Microwave electronic devices, [S. 1.], Chapter 10, Chapman & Hall, London, England, 1982, pp. 285–311.
2. E.N. Ivanov and M.E. Tobar, Low-noise microwave resonator oscillators: Current status and future developments, Bell Syst Tech J 48 (2001), 7–36.
3. K.S. Thorne, Gravitational radiation, In: S.W. Hawking and W. Israel (Eds.), 300 years of gravitation, Chapter 9, Cambridge University Press, Cambridge, England, 1987, pp. 330–445.
4. E.N. Ivanov, M.E. Tobar, and R.A. Woode, Advanced phase noise suppression technique for next generation of ultra low-noise microwave oscillators, 49th Proc 1995 IEEE Int Freq Control Symp, 1995, pp. 314–320.
5. R.A. Woode, et al., Applications of interferometric signal processing to phase-noise reduction in microwave oscillators, IEEE Trans Microwave Theory Tech 46 (1998), 1537–1545.
6. W.B. Robins, Phase-noise in signal sources, IEEE Telecommunications Series 9, Peter Peregrinus, London, 1982.
7. D.B. Leeson, Simple model of feedback oscillator noise spectrum, Proc Inst Electrical and Electronics Engineers, 54 (1966), 329–330.
8. K. Kurukawa, Some basic characteristics of broadband negative resistance oscillators, Bell Syst Tech J, 48 (1969), 1937–1955.
9. J. Duffield, Low phase-noise applications of the 8662 a and 8663, Applications Note 283-3, [S. 1]: Hewlett Packard, 1989.
10. T.J. Price, D.M. Iddles, and D.S. Cannell, Progress in the understanding, desing and processing of new and improved ceramic resonator materials, 1999 Tech Proc Filtronic Eng Conf., “Sharing Ideas”, Filtronic Pty, Baildon, West Yorkshire, 1999.
11. C.A. Flory and R.C. Taber, High performance distributed bragg reflector microwave resonators, IEEE Trans Ultrason Ferroelec Freq Control 44 (1997), 486–495.

© 2009 Wiley Periodicals, Inc.

## DESIGN OF A MICROSTIP FED STEP SLOT ANTENNA FOR UWB COMMUNICATION

M. Gopikrishna, Deepti Das Krishna, C. K. Aanandan, P. Mohanan, and K. Vasudevan

Centre for Research in Electromagnetics and Antennas, Department of Electronics, Cochin University of Science and Technology, Cochin, India; Corresponding author: anand@cusat.ac.in

Received 18 August 2008

**ABSTRACT:** The design and performance of a stepped slot printed monopole antenna in the ultrawideband is presented in this article. Multiple resonances generated by the stepped slot geometry are matched in the ultrawideband using a modified microstrip feed. The impedance bandwidth ( $SWR < 2$ ) of the antenna is from 3 to 11 GHz. Radiation patterns are stable and omnidirectional with appreciable gain throughout the band. Performance of the antenna is also analyzed in the time domain, which reveals good pulse handling capabilities. Compact geometry of the antenna allows easy commercial deployment. © 2009 Wiley Periodicals, Inc. Microwave Opt Technol Lett 51: 1126–1129, 2009; Published online in Wiley InterScience (www.interscience.wiley.com). DOI 10.1002/mop.24262

**Key words:** UWB systems; slot antennas; microwave antennas

### 1. INTRODUCTION

The widespread commercial deployment of ultrawideband (UWB) systems has sparked renewed interest in the subject of UWB

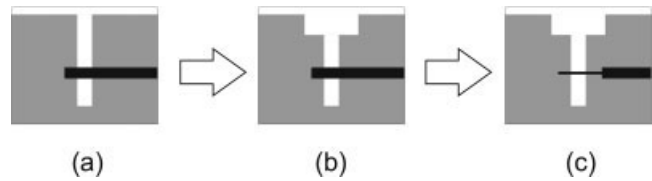


Figure 1 Design evolution of step slot antenna

antennas. An UWB system requires an antenna capable of receiving many frequencies at the same time with consistent performance across the entire band. It is also required to have a nondispersive transient characteristic. The design practice to realize ultrawide bandwidth is to generate multiple resonances and match them using appropriate techniques. In monopole radiators, step or exponential impedance inverters realized with ground and patch minimize the insidious reflections and radiate the guided signals [1–3]. There are many approaches to design a slot antenna with ultrawide bandwidth. An exponential tapered slot antenna which is excited using a broad band microstrip-slot line transition to achieve ultrawide bandwidth is reported in [4]. A coplanar waveguide is tapered to form a ring slot to accomplish ultrawide bandwidth [5]. Other designs excite a wide circular, elliptical, or rectangular slot using a stub of similar shape [6, 7].

In another class of slot radiators known as monopole slot antennas, broad banding is realized by modifying the microstrip line that excite a slot cut in the ground plane. The technique proposed in [8] uses a fictitious short circuit realized with a microstrip line of reduced width and the reported bandwidth is 32%. This concept is further studied in [9] and [10] to improve the bandwidths to 37% and 43%, respectively. The design of monopole slot antennas proposed in [11] use a wide cut in the ground plane for bandwidth enhancement and by bending the slot to “L” shape or appending an additional slot to form a “T” shape, as much as 87% bandwidth is obtained. In this article, we propose the design of a monopole slot antenna for deployment in the 3.1–10.6 GHz ultrawideband. To create multiple resonances, the slot in the ground plane is designed with a staircase shape. These resonances are matched using a modified feed structure. In addition to the wider impedance bandwidth and excellent radiation characteristics, the proposed design is simple and compact compared with the previous designs. A detailed account of this design is presented in Section 2. Performance of the antenna is analyzed in the frequency as well as the time domains and the results are presented in Section 3.

### 2. ANTENNA DESIGN

Design evolution of the monopole step slot antenna is shown in Figures 1(a)–1(c). The monopole slot designed at the bottom of the dielectric substrate is excited using an open end microstrip feed at the top. The design in Figure 1(a) exhibits a dual band behavior with widely separated resonances as indicated in Table 1, in which the first resonance is due to the open slot at the edge and the second resonance is due to the aperture formed below the microstrip feed line. To create additional resonances in between, the open slot in the ground plane is made step like as shown in Figure 1(b). Finally, to match these resonances, width of the microstrip line is reduced

TABLE 1 Antenna Designs and the Observed Resonances

Antenna	Resonances
a	3.62, 9.18 GHz
b	3.65, 5.78, 10.31 GHz
c	3.58, 5.18, 8, 10.31 GHz

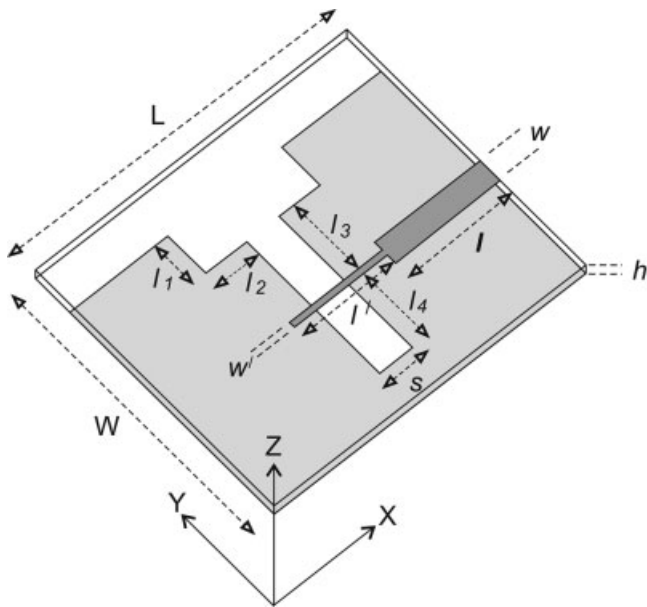


**Figure 2** Geometry of the monopole step slot antenna

at the microstrip-to-slot line transition. Geometry of the final design is shown in Figure 2. From an analysis of this design in HFSS, it is found that there is resonance in the antenna for different combinations of lengths  $l_2$ ,  $l_3$ , and  $l_4$ . The first resonance satisfies a half wave variation which can be expressed as,

$$l_2 + l_3 + l_4 + w' = 0.5\lambda_{d1} \quad (1)$$

The second resonance is due to the half wave variation,

$$l_2 + l_3 + w' = 0.5\lambda_{d2} \quad (2)$$

For the third resonance,

$$l_3 + w' = 0.5\lambda_{d3} \quad (3)$$

For the fourth resonance,

$$l_4 = 0.5\lambda_{d4} \quad (4)$$

**TABLE 2** Computed Geometric Parameters for the Antennas

Laminate	Antenna 1	Antenna 2	Antenna 3
	Taconic RF-30	FR4 Glass epoxy	Rogers RO3006
$\epsilon_r$	3	4.4	6.15
$\tan \delta$	0.0013	0.02	0.002
$H$ (mm)	1.52	1.6	1.28
$l_1$ (mm)	5.5	5.5	5.5
$l_2$ (mm)	5.4	5.35	4.8
$l_3$ (mm)	11.9	10.15	9.9
$l_4$ (mm)	9.4	8.65	7.8
$L$ (mm)	15.5	13.5	14.2
$l'$ (mm)	14	12	10.7
$w$ (mm)	3.8	3	1.9
$w'$ (mm)	1.2	0.7	0.4
$s$	4	4	4
$L \times W$	$46 \times 35$	$40 \times 32$	$38 \times 28$

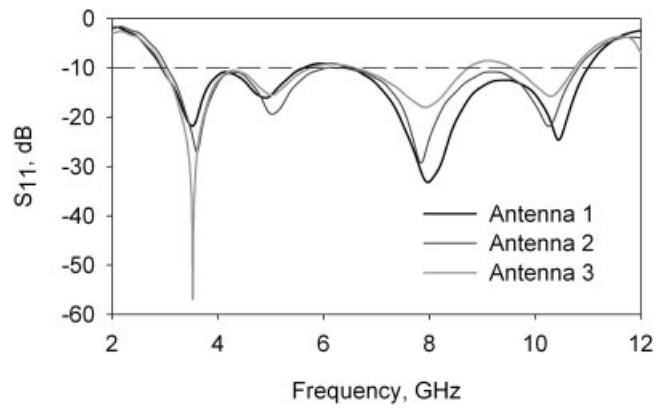


**Figure 3** Return loss of antennas indicated in Table 2

Here,  $\lambda_{di} = \lambda_{0i} / \sqrt{\epsilon_{re}}$  where  $i = 1, 2, 3, 4$ ;  $\lambda_{0i}$  is the free space wavelength computed at the resonance and  $\epsilon_{re} = (\epsilon_r + 1)/2$ . The microstrip to slot line transition is designed with a reduced width  $w'$  to match these resonances. The validity of these equations is studied by designing the antenna on laminates with different permittivity and the parameters are given in Table 2. Impedance bandwidths of these antennas are plotted in Figure 3. Simulation studies reveal that  $l_1$  does not affect the resonances in the antenna; but, overall matching can be slightly improved by decreasing  $l_1$  as the permittivity increases. Likewise, parameters  $s$ ,  $W$ , and  $L$  do not affect resonances in the antenna and the values given in Table 2 ensure good radiation characteristics. Electric field in the conductor (intensity plot) and the aperture field (vector plot) at these frequencies are shown in Figure 4, which further validates the above analysis.

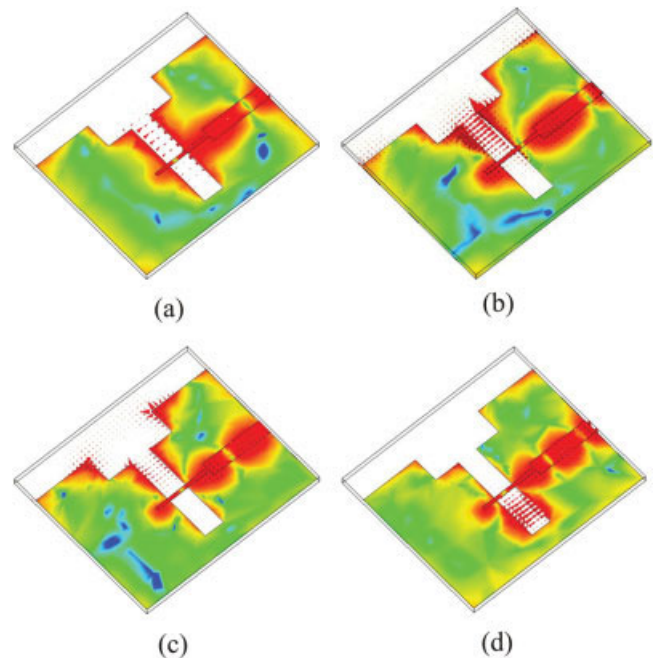


**Figure 4** E-field distribution on the conductor (Intensity) and aperture (vector) at (a) 3.58 GHz, (b) 5.18 GHz, (c) 8 GHz, and (d) 10.37 GHz. [Color figure can be viewed in the online issue, which is available at [www.interscience.wiley.com](http://www.interscience.wiley.com)]

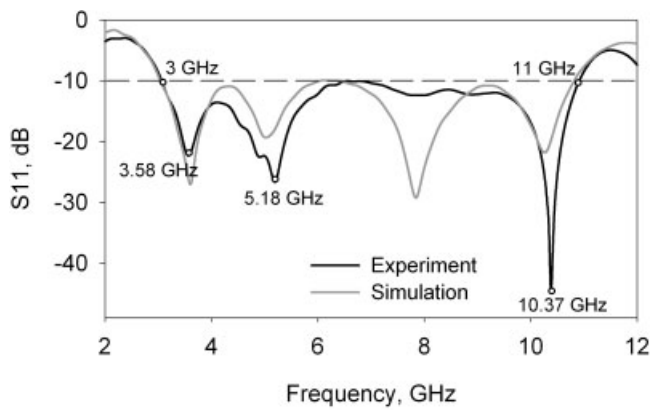


Figure 5 Measured and simulated return losses of Antenna 2

### 3. EXPERIMENTAL RESULTS AND DISCUSSION

#### 3.1. Frequency Domain Analysis

A prototype of the antenna is fabricated on glass epoxy substrate with parameters given in Table 2 and the measurements were performed using R&S ZVB 20 VNA. Figure 5 shows the measured and simulated return loss characteristics of this antenna. The  $-10$  dB bandwidth of the antenna is from 3 to 11 GHz, which covers the band for UWB communication and measurement applications.

Simulation studies indicate that matching at the higher resonance is dependent on parameter  $w'$ .

Measured radiation patterns of the antenna in the  $Y-Z$ ,  $X-Z$ , and  $X-Y$  planes at three different frequencies are shown in Figure 6 along with the simulated results. Across all planes, radiation remains approximately omni directional with polarization in the  $X$ -direction. Average value of cross polarization is  $-20$  dB except in the  $X-Z$  plane, which shows high cross polar radiation throughout the band. An explanation for this can be arrived from the electric field distribution shown in Figure 4, which shows the presence of a  $Y$ -component for the field because of its fringing in the aperture. The average gain in the 3.1–10.6 GHz band is observed to be 3.16 dBi. The gain measurements show reasonable agreement with simulation as shown in Figure 7.

#### 3.2. Time Domain Analysis

For the time domain measurements, two identical prototypes are used as transmitter and receiver, which are kept apart in the far field. To study the far field phase linearity of the transmitted signals, group delay measurements were performed using the VNA. As shown in Figure 8, the delay remains constant for the side-by-side orientation, whereas the face-to-face orientation shows variation at 7 GHz. This variation can be due to the slight distortion observed in the radiation pattern resulted from an uneven mode transition in the antenna. To measure the transient response, the antenna is modeled by its transfer function with the

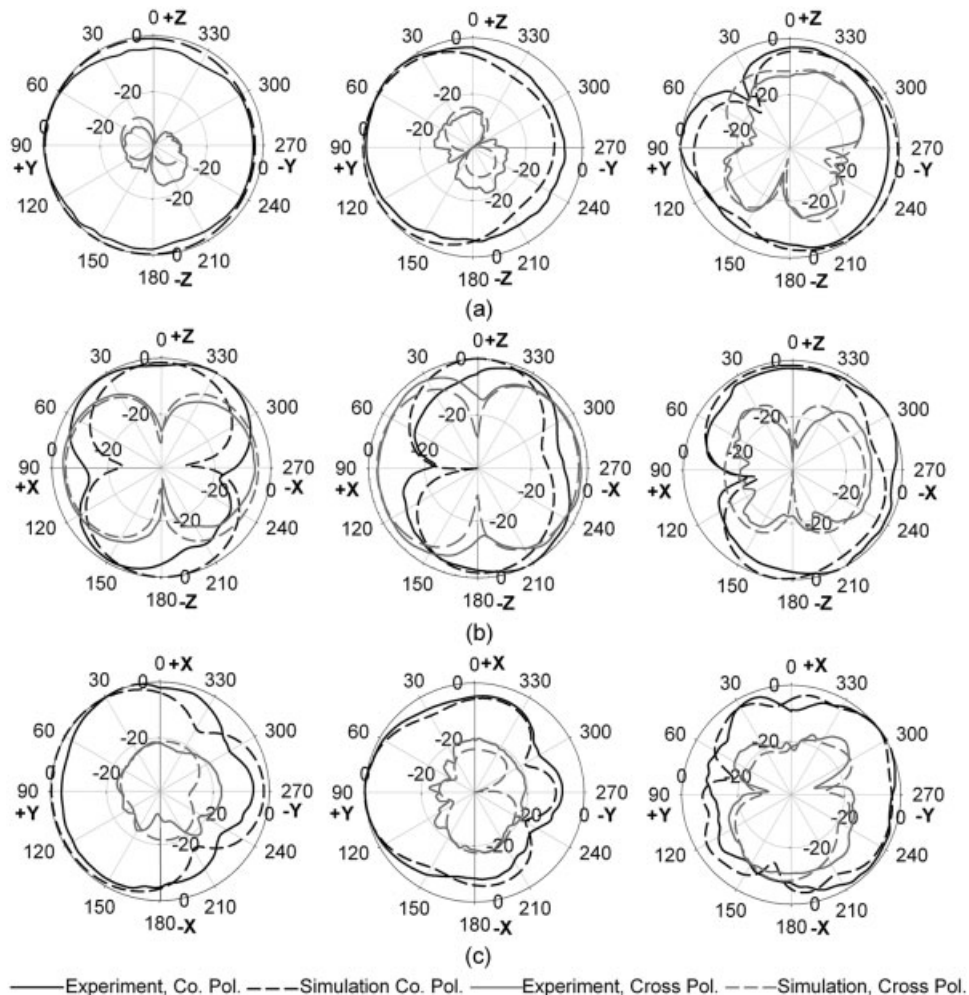


Figure 6 Radiation patterns of the antenna at 3.58 GHz, 5.18 GHz, and 10.37 GHz. (a)  $Y-Z$  plane, (b)  $X-Z$  plane, (c)  $X-Y$  plane

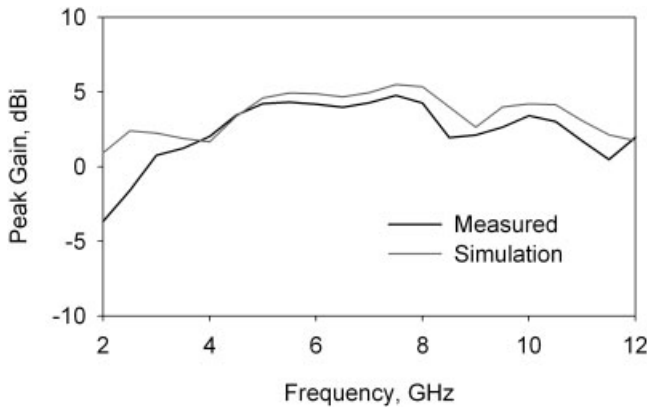


Figure 7 Measured and simulated peak gains of Antenna 2

transmission coefficient  $S_{21}$  measured in the frequency domain for side-by-side and face-to-face orientations. From this, the antenna transfer function is computed as [2, 3],

$$H(\omega) = \sqrt{\frac{2\pi R c S_{21}(\omega) e^{j\omega R/c}}{J\omega}} \quad (5)$$

where  $c$  is the free space velocity and  $R$  is the distance between the two antennas. This is convoluted with the spectrum of the input pulse,

$$v_{in}(t) = A \sin(2\pi f_c t) \cdot e^{-(t/T)^2} \quad (6)$$

Here,  $A = 1.61$  and the pulse duration parameter  $T = 90$  ps. The measured antenna transfer function is also represented in Figure 9 for the two orientations of the antenna with  $R = 45$  cm. In Figure 9, the input and received waveforms are shown. The input pulse is scaled by 0.02 for easy comparison with the received waveforms. Maximum magnitude of the waveform for the face-to-face orientation is found to be less than the side-by-side orientation. The dispersion caused by the geometry of the antenna to the input signal is minimal in this design.

#### 4. CONCLUSIONS

It has been demonstrated that ultrawide bandwidth can be realized with a stepped slot design excited using a modified microstrip feed. The proposed radiator provides omnidirectional coverage with appreciable gain throughout the band. The antenna also shows good performance with minimal dispersion and ringing to the transmitted pulse. Also, the design is simple and compact for integration with circuitry and hence is a suitable candidate for portable UWB applications.

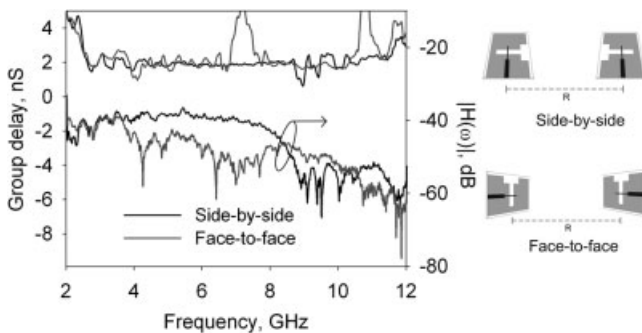


Figure 8 Measured group delay and antenna transfer function

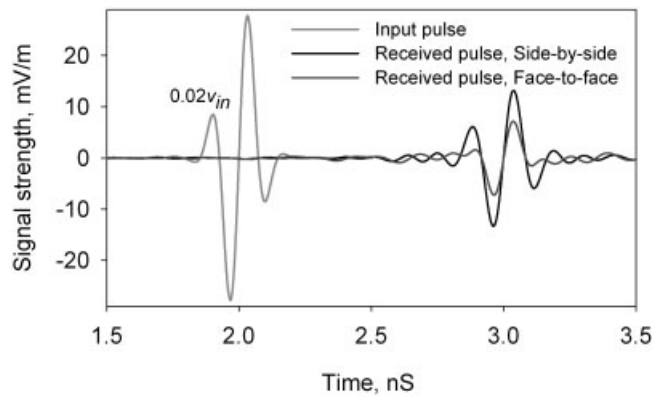


Figure 9 Input and received pulses

#### ACKNOWLEDGMENTS

M. Gopikrishna and Deepti Das Krishna acknowledge the University Grants Commission, India and the Department of Science and Technology, Govt. of India, respectively, for providing financial assistance for their research work. Measurements were carried out using the facilities created under DST-FIST program.

#### REFERENCES

1. Y.J. Cho, K.H. Kim, D.H. Choi, S.S. Lee, and S.O. Park, A miniature UWB planar monopole antenna with 5-GHz band-rejection filter and the time-domain characteristics, *IEEE Trans Antennas Propag* 54 (2006), 1453–1460.
2. M. Gopikrishna, D.D. Krishna, A.R. Chandran, and C.K. Anandan, Square monopole antenna for ultra wide band communication applications, *J Electromagn Waves Appl* 21 (2007), 1525–1537.
3. D.D. Krishna, M. Gopikrishna, C.K. Anandan, P. Mohanan, and K. Vasudevan, Planar elliptic ultra wide band antenna with band notch characteristics, *Int J Wireless Opt Commun* 4 (2007), 1–12.
4. I.-J. Yoon, H. Kim, K. Chang, Y.J. Yoon and Y.-H Kim, Ultra wideband tapered slot antenna with band-stop characteristic, *IEEE Antennas Propag Soc Int Symp* 2 (2004), 1780–1783.
5. T.G. Ma and C.H. Tseng, An ultra wideband coplanar waveguide-fed tapered ring slot antenna, *IEEE Trans Antennas Propag* 54 (2006), 1105–1111.
6. E.S. Angelopoulos, A.Z. Anastopoulos, D.I. Kaklamani, A.A. Alexandridis, F. Lazarakis, and K. Dangakis, Circular and elliptical CPW-fed Slot and microstrip-fed antennas for ultrawideband applications, *IEEE Antennas Wireless Propag Lett* 5 (2006), 294–297.
7. Y.C. Lin and K.J. Hung, Compact ultra wideband rectangular aperture antenna and band-notched designs, *IEEE Trans Antennas Propag* 54 (2006), 3075–3080.
8. L. Zhu, R. Fu, and K.L. Whu, A novel broadband microstrip-fed wide slot antenna with double rejection zeros, *IEEE Antennas Wireless Propag Lett* 2 (2003), 194–196.
9. N. Behdad and K. Sarabandi, A wide-band antenna design employing a fictitious short circuit concept, *IEEE Trans Antennas Propag* 53 (2005), 475–482.
10. N. Behdad and K. Sarabandi, A multiresonant single-element wide band slot antenna, *IEEE Antennas Wireless Propag Lett* 3 (2004), 5–8.
11. S.I. Latif, L. Shafai, and S.K. Sharma, Bandwidth enhancement and size reduction of microstrip slot antennas, *IEEE Trans Antennas Propag* 53 (2005), 994–1003.

© 2009 Wiley Periodicals, Inc.